Journal of Pharmaceutical, Chemical and Biological Sciences
ISSN: 2348-7658
CODEN: JPCBBG
Impact Factor (GIF): 0.701
Impact Factor (SJIF): 3.905
September- November 2017; 5(3):221-230
Published on: October 26, 2017

Research Article

Synthesis, Characterization and Anti-Microbial Activities on Polyaniline-$CdTiO_3$ Nanocomposite

P. Suja Prema Rajini[1], V. S. John[1*], R. Murugesan[2]

[1]Department of Physics, Tirunelveli Dakshina Mara Nadar Sangam College, T. Kallikulam, Tirunelveli District 627113, Tamil Nadu, India.
[2]Department of Chemistry, Tirunelveli Dakshina Mara Nadar Sangam College, T. Kallikulam, Tirunelveli District 627113, Tamil Nadu, India

***Corresponding Author:** V. S. John, Department of Physics, Tirunelveli Dakshina Mara Nadar Sangam College, T. Kallikulam, Tirunelveli District 627113, Tamil Nadu, India.

Received: 05 September 2017 **Revised:** 06 October 2017 **Accepted:** 08 October 2017

ABSTRACT

Conducting polyaniline-inorganic nanocomposite (PINC) is applied in various fields via electrotherapy, electro-magnetic materials for monitoring health, antimicrobial clothing, data transfer in smart textiles, biosensors and for defence technology. In the present study, polyaniline (Pani) and its nanocomposites with TiO_2 and $CdTiO_3$ in 1 M H_2SO_4 medium were prepared using ammonium perdisulphate (APS) as an oxidizing agent. The polymerization yield was noted. The conductivities of the samples were measured by four probe method. The spectral properties of EPR, UV-Visible and FTIR were studied to confirm the chemical structure of Pani and its nanocomposites. The sharp peaks in the XRD show that Pani-SO_4^{2-}/TiO_2 and Pani-SO_4^{2-}/$CdTiO_3$ have enhanced crystallinity. The particle size was evaluated using Debye-Scherrer's formula and the average crystalline size of Pani-SO_4^{2-} and its nanocomposites were found to be 53, 46 and 42 nm, respectively. The SEM studies were supported that the polymer samples were in homogeneity. The polymer samples were examined for antibacterial activities against Gram positive and Gram negative bacteria such as more activity against *Streptococcus faecalis* and *Bacillus subtilis* and lesser activity against *Klebsilla pneumonae*, *Escherichia coli*, *Proteus vulgaris* and *Pseudomonas aeruginosa* comparative to standard chloramphenicol. The antibacterial activities were evaluated by measuring the zone of inhibition. It is found that Pani-SO_4^{2-}/$CdTiO_3$ has higher antimicrobial activity than Pani-SO_4^{2-} and Pani-SO_4^{2-}/TiO_2. This information is useful to the potential application of nanocomposites in fabrics incorporated with antibacterial agents as a prophylactic use against bacterial skin infections in the near future.

Keyword: Polyaniline; nanocomposite; conductivity; spectral properties; anti-microbial activity

INTRODUCTION

Various PINC synthesised at different combinations of components have progressive interest in recent years due to their significant properties and applications [1, 2]. Thus, the combination of polyaniline (Pani) with inorganic material such as semiconductor nanoparticle is gaining importance because Pani has good processibility, ease of preparation, cost effectiveness, environmental stability and potential application in the field of catalysis, photocatalysts, biosensors, batteries, electronics,

opto-electronics and enable particle size control which leads to uniform distribution of nanoparticles [3, 4]. Considering the significant properties, it is used to synthesis of heterostructure Pani-nanocomposites. These nanocomposites play an important role in the fabrication of electronic devices which combine superior electronic, magnetic and optical properties [5-7]. Due to the wide range of band gap, TiO_2 act as a competent photo-catalyst. The several reports describe the synthesis of photoactive nanocomposite of Pani with semiconductor of TiO_2 such as Pani/TiO_2, Pani/$BiVO_4$ [8], Pani/SiO_2 [9], Pani/SnO_2 [10], Pani/CdS [11], Pani/V_2O_5 [12] and Pani/Fe_3O_4/SiO_2/TiO_2 [13].

Previous researchers illustrate that the properties of Pani/TiO_2 nanocomposite are reasonably different from Pani and TiO_2, which ensures the strong interaction between two components [14-16]. The antibacterial properties of photocatalyst Pani/TiO_2 are important for environment and health care industries. Pani/TiO_2 nanocomposites have good antibacterial properties [17] especially on *Staphylococcus aureus* and *Escherichia coli*.

Several current reports are, improving Pani as a sensitivity and selectivity with preparation of nanostructured forms [18, 19] with addition of metal oxide. Such nanocomposite operates and the selectivity towards different gas species is controlled by volume ratio of nanosized metal oxide. The properties of nanocomposite depend not only on the properties of their constituents but also on the morphology and interfacial characteristics [20]. The nanostructured metal oxides are promising new material for blending with polymers, which has an excellent mechanical, electrical, thermal and multifunctional properties. It is fascinating to develop an inexpensive, facile and fast method in the preparation of single phase binary metal oxides. The synthesis of binary metal oxide polymer nanocomposites exhibits the following advantages: good chemical homogeneity, simple equipment and preparation process, inexpensive raw materials, etc.

The present work deals with synthesis and physico-chemical properties of nanostructurized PINC. The material of PINC has been improved by modifying with inorganic semiconducting binary metal oxides. Water-soluble green synthesized binary metal oxides are novel candidates for dopants. In the present case, binary metal oxides of Ti (IV) and Cd (II) are to be green synthesised and incorporated into Pani during *in-situ* polymerisation of aniline by using ammonium perdisulphate (APS) as an oxidant in aqueous 1 M H_2SO_4. The nanocomposites have entirely different characteristics from conventional inorganic dopants of mineral acids, the resulting PINC have a good chance to possess new properties.

EXPERIMENTAL

Preparation of polyanilinecadmium-titanate (Pani-SO_4^{2-}/$CdTiO_3$) nano-composites

The 0.1 M aniline in aqueous 1 M H_2SO_4 in the presence of binary metal oxides of $CdTiO_3$ was chemically polymerised [21] by using drop-wise addition of 0.1 M APS as oxidizing agent at constant stirring for half an hour. After addition of APS, polymerization was allowed to proceed further for overnight in a refrigerator. The polymer sample was filtered, washed with water, then methanol and acetone until the filterate became colourless and dried in an air oven at 80°C for about 4 hours. The dried polymer sample was ground into a fine powder and the yield was noted. The sample was stored in air-proof sealed plastic covers. On comparative study, the materials of polyaniline sulphate (Pani-SO_4^{2-}) and its nanocomposite with TiO_2 (Pani-SO_4^{2-}/TiO_2) were prepared in identical conditions.

Characterization of polymer materials

The polymer samples were made as pellets with hydraulic pressure and used to measure conductivity. The current-voltage (I-V) characteristics were measured by four probe set-up at room temperature. EPR spectra were recorded from Varian E-112 ESR spectrometer (RSIC, IIT Madras) operating in the X-band, scan 50 gauss, time constant 0.5 sec, modulation amplitude 3.2 gauss, field set 3200 gauss, microwave power 20mW, modulation frequency 100kHz, microwave frequency 9.46 GHz, at room temperature and 1,1̇-diphenyl-2-picrylhydrazyl (DPPH) as a reference material. The UV-Visible spectra of NMP or m-cresol dissolved polymer samples were recorded using UV/VIS/NIR Spectrometer from 300 to 1100 nm in quartz cell. FTIR spectra of polymer samples in KBr pellet were recorded on computer-controlled FTIR

spectrophotometer in 400-4000 cm^{-1} at the resolution of 4 cm^{-1}. The structural properties of the samples were studied by using X-ray diffractometer (XRD) with CuKα radiation, having λ=1.5406 Å. The morphological studies were recorded by using SEM with gold coated.

Studies of anti-microbial activity

The antibacterial activity of the polymer materials (Pani-SO_4^{2-}, Pani-SO_4^{2-}/TiO_2, Pani-SO_4^{2-}/$CdTiO_3$) were evaluated *in-vitro* against eight bacteria: *Escherichia coli*, *Staphylococcus aureus*, *seudomonas aeruginosa*, *Proteus mirabilis*, *Enterobacter sps, Chromobacter, Proteus vulgaris and Klebsiella pneumonia* strains using disc diffusion method. The bacteria were plated onto solid nutrient agar. 100 µL of the test solution sample was used into each of the poured wells on the plates; incubation at 22-25 ± 2°C for 24 hours, the zone inhibition was recorded. The solvent NMP used as a negative control, whereas the antibiotic of Chloramphenicol used as a positive control.

RESULTS AND DISCUSSION

Preparation of Pani and its nanocomposites

The chemical polymerization of aniline in the presence or absence of colloidal solution of TiO_2 or $CdTiO_3$ was prepared in aqueous 1 M H_2SO_4 medium and using APS as oxidising agent. The polymerisation yield of Pani and its nanocomposites with TiO_2 and $CdTiO_3$ are reported in the Table 1. The incorporation of metal oxides in the Pani samples, the yield is enhanced as compared with Pani-SO_4^{2-} sample. The results indicate that the incorporation of binary metal oxide enhances the polymerization yield as well as the rate of reaction or the growth of polymerization chain. Several studies are supported this behaviour. In $CdTiO_3$, the polymerization yield increases, compared with TiO_2. This indicates that the activity of TiO_2 has enhancing tendency by the addition of Cd^{2+} ions.

Table 1: Polymerization yield, conductivity, EPR and UV-Vis Spectral data of polymer samples

Sample	Yield (g)	Conductivity	EPR spectral data			UV-Vis spectral data	
			g	Width (gauss)	A/B Ratio	NMP	m-Cresol
Pani-SO_4^{2-}	1.192	0.9029	2.02	178.57	0.952	539, 984	401, 578, 752, 973
Pani-SO_4^{2-}/TiO_2	1.576	1.8125	2.02	249.99	0.777	542, 982	399, 579, 756, 975
Pani-SO_4^{2-}/$CdTiO_3$	1.772	2.0565	1.99	281.12	0.333	538, 980	401, 581, 755, 970

Conductivity

Polymer samples were made as pellets and subjected to D. C. conductivity measurements in a four probe set-up. Current and voltage measurements of the samples were made at different positions of the pellet, in which values were more or less the same value within the experimental error. Conductivity values were then computed from the values of resistance and dimensions of the samples using the following equation:

$$\text{Conductivity } (\sigma) = (1/R) \times (1/2\pi s)$$

Where R is the resistance and s = 2nm is the distance of the two probes.

The current and voltage values were plotted and the resistances were obtained from the slope of the plots. The calculated conductivity of polymer samples is given in the Table 1. The metal oxide nanoparticles are incorporated into Pani to form nanocomposite. The nanocomposites properties are extremely sensitive to small changes in content due to the size and shape of metal oxide incorporated into polymer-inorganic nanocomposites [22]. The increase in conductivity of the PINC contain metal oxide as filler nanoparticle due to the formation of more number of polarons in the wider band gap, which is also confirmed by UV-Visible spectra. The change in conductivity of nanocomposite indicates a change in the doping level of Pani. The nanocomposite of binary metal oxide shows the higher conductivity than Pani. The enhancement of conductivity values is attributed to uncoiling of polymeric chains due to strong interfacial interaction between binary metal oxides with Pani caused by their composition [23]. In this fact is supported by other characterization of EPR, UV-Visible, FTIR spectral, X-ray diffraction and SEM studies.

EPR studies

The results of EPR study on doped Pani nanocomposites with TiO_2 and $CdTiO_3$ are presented in the Table 1. In Pani, display a single resonance isotropic line with g value of 2.01 which is assigned to the presence of non-spin paired (S = ½) polaron [24]. The Pani-SO_4^{2-} exhibits the values of g, which is close to the free electron g value of 2.0023 indicative of resonance that comes from electron delocalized in the π-system of carbon atoms forming the polymer back bone in the main chain. When TiO_2 contents increases, the asymmetry signal is more broadened. In Pani nanocomposites the width line of ΔH depends on TiO_2 and $CdTiO_3$ values of g, which close to Pani-SO_4^{2-}. It indicates that the polarons in the Pani-SO_4^{2-}/TiO_3 and Pani-SO_4^{2-}/$CdTiO_3$ are more delocalized than in Pani-SO_4^{2-}. In the photo-excitation process charges are transferred from Pani to TiO_2 and $CdTiO_3$ which contribute strong electronic interaction between two components. It is possible to a strong interchange of electrons between the nitrogen atom and benzene ring in the polymer chain.

UV-Visible spectral studies

The UV-Visible spectra of Pani-SO_4^{2-} (curve 1), Pani-SO_4^{2-}/TiO_2 and Pani-SO_4^{2-}/$CdTiO_3$ (curve 2, 3) dissolved in NMP are given in Fig.1 and their peak positions are reported in Table 1. The result indicates that Pani-SO_4^{2-} is completely transformed from the emeraldine salt to the emeraldine base by the deprotonation of Pani-SO_4^{2-} with NMP as co-ordinate solvent. The absorption band around 200-300 nm conjugated system and π-polaron band around 500-750 nm gradually disappeared in the Pani-SO_4^{2-} samples spectra and the band around 540 nm emerged. The absorption band at 540 nm is attributed to the excitation of transition from the highest occupied molecular orbital of the benzenoid to the lowest unoccupied molecular orbital of the quinoid ring and the two surrounding imine nitrogens in the emeraldine base form of Pani-SO_4^{2-}.

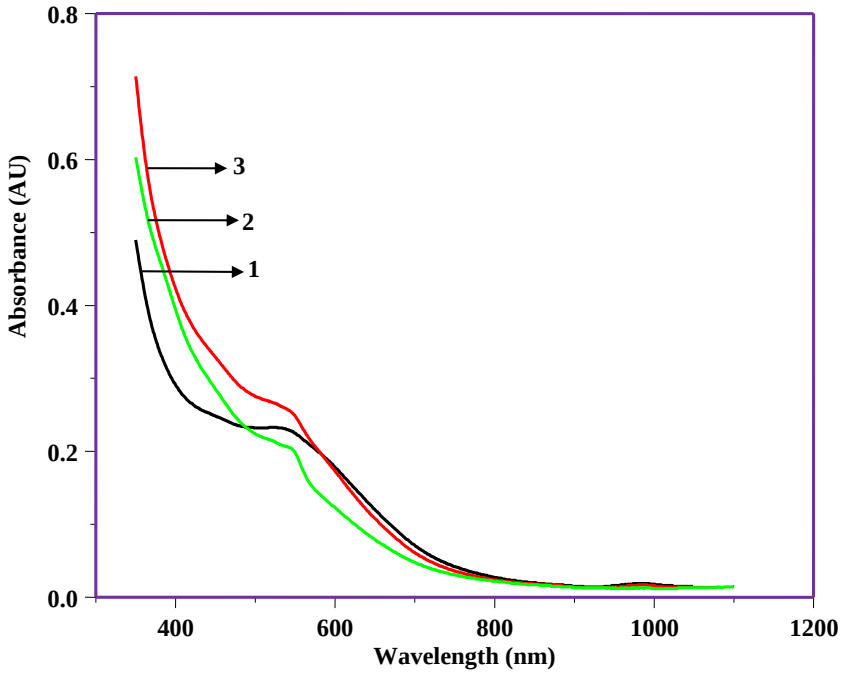

Fig.1 UV-Visible spectra for
(1) Pani-SO_4^{2-}; (2) Pani-SO_4^{2-}/TiO_2 and (3) Pani-SO_4^{2-}/$CdTiO_3$ in NMP solvent

Furthermore, when metal oxide nanoparticles are dispersed in the Pani-SO_4^{2-} matrix, a significant change is measured in the absorption spectra. The red shift of absorption transition to higher wavelength is due to the successful interaction of metal oxide with the polymer chain. The characteristic features of absorption spectra indicate that Pani-SO_4^{2-}/TiO_2 and Pani-SO_4^{2-}/$CdTiO_3$ nanocomposites are in the conducting state. In fact, the synthesized Pani-SO_4^{2-} is in the protonated form, the absorption

band of the transition of benzenoid rings into quinoid rings is more than 500 nm.

This is due to the presence of hydrogen bonding interaction of C=O group in NMP with the NH group in Pani-SO_4^{2-}. Since the C=O group interact or form hydrogen bond with the dopant, which prevent the Pani from acid-doping [25]. This is confirmed by a broad absorption band near 540 nm in the UV-Visible spectra of Pani-SO_4^{2-}. To compare, the curve (2, 3) with curve (1) in Fig.1, the peak of quinoid ring transition, shifts from 485 to 540 nm when TiO_2 and $CdTiO_3$ added into Pani-SO_4^{2-}. The reason indicate that 'compact coil' of Pani with nanocomposite chain make the energy gap of quinoid ring transition narrower, thus transition of electrons becomes easier.

The UV-Visible spectra of Pani-SO_4^{2-}, Pani-SO_4^{2-}/TiO_2 and Pani-SO_4^{2-}/$CdTiO_3$ nanocomposites in m-cresol as solvent are shown in Fig.2. These samples show four characteristic absorptions at 400, 580, 750 and 970 nm wavelength. The first absorption band is attributed to π-π* electron transition within benzenoid segments. The second and third absorption bands should be related to doping level and formation of polaron and fourth one is extended head-tail polymer chain respectively [26]. Fig.2 show that the entire characteristic peaks of Pani-SO_4^{2-} appears in Pani-SO_4^{2-}/TiO_2 and Pani-SO_4^{2-}/$CdTiO_3$ nanocomposites. The first three distinctive peaks almost same, obviously, two peaks at 400 and 580 nm almost coalesce together into a single peak. This indicates that the presence of nanoparticle has some effect on the conjugated structure of the conducting Pani. In addition, the peak intensity over 970 nm corresponding to π-π* transition of benzenoid segments, which is related to the number of repeating units of monomer in Pani chain, was increased after addition of TiO_2 and $CdTiO_3$.

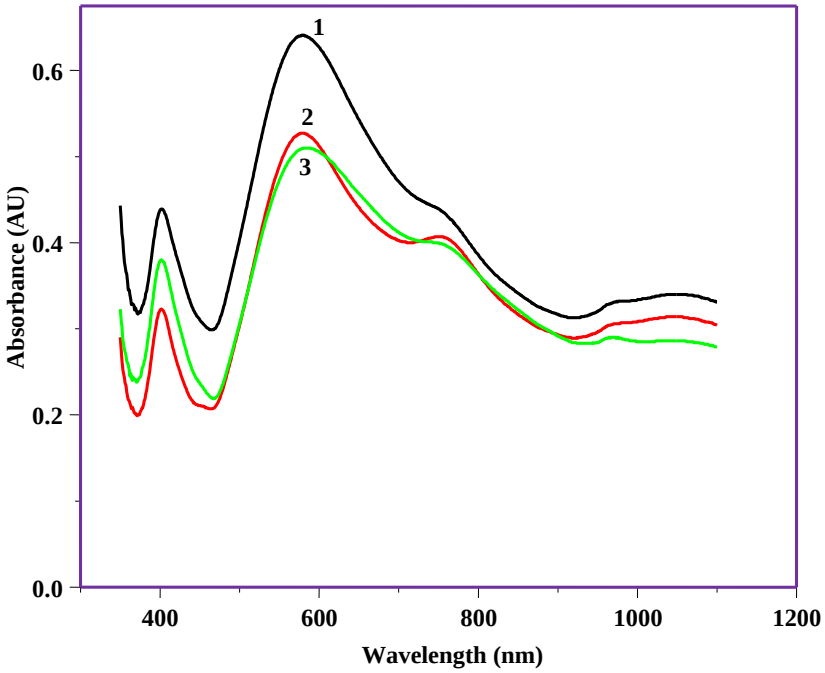

Fig.2 UV-Visible spectra for
(1) Pani-SO_4^{2-}; (2) Pani-SO_4^{2-}/TiO_2 and (3) Pani-SO_4^{2-}/$CdTiO_3$ in m-cresol solvent

FTIR spectral studies

The general formula for Pani materials in their base forms consists of three benzenoid (–C_6H_4 NH–NH–) units denoted as B and one quinoid (–N=C_6H_4=N–C_6H_4) unit denoted as Q. It is written as [(B–B)y(Q–B)1–y]n. The *y* value accounts to the oxidation state of the polymer, leucoemeraldine (completely reduced, *y* = 1), emeraldine salt (half reduced, *y* = 0.5) and pernigraniline salt (completely oxidized, *y* = 0) states [27-29].

The principal characteristic peaks of quinoid-benzenoid N moieties, C-N stretching, C-H aromatic in-plane and out-plane bending

vibrations of Pani are observed to occur at about 1600, 1500, 1350, 1130 and 820 cm^{-1}, respectively [30]. In the present study, all these peaks are observed in Pani-SO_4^{2-} but are modified both in intensity and peak position on doping with TiO_2 and $CdTiO_3$. These changes indicate the structural and chemical modifications of Pani by TiO_2 and $CdTiO_3$. For example, the intensity of C-$N^{\oplus}$ stretching doublet band (1350 cm^{-1}) [31] is enhanced very much relative to TiO_2 and $CdTiO_3$ nanocomposites than with SO_4^{2-} alone. Moreover, in TiO_2 and $CdTiO_3$ doped Pani materials, the doublet splits into a triplet and shifts to lower wave number, 1300 cm^{-1}. This observation demonstrates that in Pani materials, the C-N group vibration is facilitated due to its greater promotion and/ or degree of exposure, their inclusion in and strong interaction with Pani to create additional C-$N^{\oplus}$ groups (structural change). It enhance the polymer chain length (conformational change) leading to exposure of the hidden C-$N^{\oplus}$ groups. Previous works [32-34] have reported that the relative concentration of various N moieties; NH, $^{\oplus}NH_2$, N=, $^{\oplus}$NH=, C=$N^{\oplus}$– in Pani depends on the nature and percentage of doping which in turn affect the population of charge defect centres (polaron and bipolaron) and ultimately the conductivity.

In comparison with the Pani and its nanocomposites, it has narrower and sharp peaks indicated that all the Pani nanocomposite, the molecular orientation is ordered. The intensity and position of the absorption band changed obviously. The C=C stretching vibration of benzenoid and quinoid units became stronger. The relative absorption band at 1576 and 1476 cm^{-1} shift change in Pani nanocomposites. The other peaks are occurred red shift due to the close packing of molecules. Especially the characteristic peak of doped Pani at 1081 cm^{-1} shifts to lower frequency. This change is indicated to derive from the ordered organization. The absorption band at 1125 cm^{-1} gradually shifts to higher frequency with the ordered extent. These results are all due to the change from ordered to disorder one. 1300 and 1006 cm^{-1} bands are assigned to C-N stretching and C-H in-plane bending vibrations, respectively. The increase in their intensities probably involved in the molecule close arrangement. In addition, there is a new small peak at 1372 cm^{-1} that is assigned to the C=N stretching vibration in quinoid unit of Pani intrinsic state.

FTIR data (Table 2) clearly indicates that the Pani incorporated inorganic binary metal oxides have strong binding with polymer host molecules. The charge delocalization peaks of inorganic nanoparticles doped Pani enhances intensities and split singlet peak into doublet or triplet due to strong interaction between inorganic dopant and Pani backbone chain. This clearly indicates that all the inorganic semiconducting or conducting materials are incorporated into polymer host matrix to increases its electrical conductivity.

Table 2: FTIR spectral data for polyaniline nanocomposite materials

Characteristic FTIR peaks for Polyaniline	Pani-SO_4^{2-}	Pani-SO_4^{2-}/TiO_2	Pani-SO_4^{2-}/$CdTiO_3$
C-H out-plane bending vibrations	881	881	851, 881
C-H in-plane bending vibrations	1081	1082	1010, 1068
Charge polymerization peaks	1128	1166	1170
The C=N stretching vibration in quinoid	1300	1296	1236, 1290
The C=C stretching vibration of benzoid	1476	1477	1402
The C=C stretching vibration of quinoid	1576	1568	1608

XRD studies

Powder XRD results of the polymer samples are shown in Fig.3. The patterns do not show any sharp peak and suggest generally an amorphous nature to all the polymer samples. However, the polymer samples display diffuse broad peak at 2θ ranging from 24° to 27°. The d-spacing was calculated from the 2θ value and is reported to be the characteristic distance between the ring planes of benzene ring in adjacent chains and is also said to be the interchain distance or the close contact distance between two adjacent chains. Further, it is a general observation that the polymer chain array and interchain distance

are affected by the size and shape of interlying dopants which results an increase in electron polymerization length when the dopants are of large size [35].

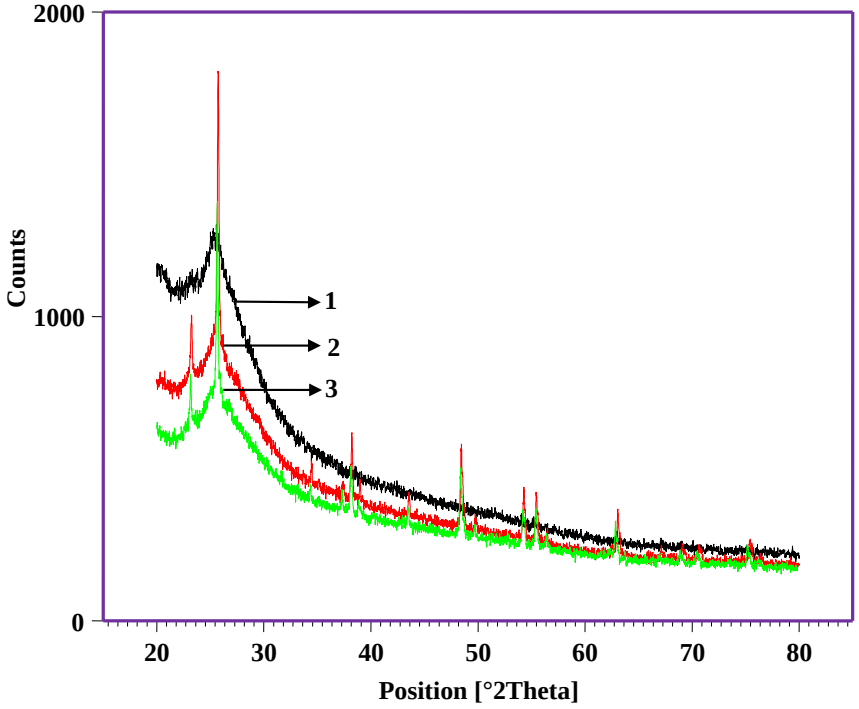

Fig.3 XRD pattern for
(1) Pani-SO_4^{2-}; (2) Pani-SO_4^{2-}/TiO_2 and (3) Pani-SO_4^{2-}/$CdTiO_3$

The d-spacing values are higher in all polymer nanocomposites as compared with Pani-SO_4^{2-} salt. The metal oxide dopants have larger size than SO_4^{2-}, its inclusion is more probable to increase the interchain distance and consequently the charge polymer length. This is a very crucial and favourable factor to have higher conductivity value. The particle size was estimated using the Debye-Scherrer formula as

$$D = 0.96\lambda / \beta \cos \theta$$

Where, $\beta \rightarrow$ The width of XRD pattern line at half peak-height (Rad)

$\lambda \rightarrow$ The wavelength of X-ray (1.5056 Å)

$\theta \rightarrow$ The angle between the incident and diffraction beam (°)

$D \rightarrow$ The particle size of the sample (nm)

The calculated crystalline sizes with different peak values and the average crystalline size of Pani-SO_4^{2-}, Pani-SO_4^{2-}/TiO_2 and Pani-SO_4^{2-}/$CdTiO_3$ nanocomposites are found to be 56.61 nm, 48 nm and 40.23 nm, respectively. This is observed that condensed particle size of nanocomposites of Pani is due to the insertion of metal oxide of TiO_2 and $CdTiO_3$.

Morphology (SEM) Studies

Fig.4 illustrates the scanning electron micrographs of the Pani-SO_4^{2-} and its nancomposites of TiO_2 and $CdTiO_3$ revealing that their production of composites were successfully achieved yielding materials with particles size well dispersed within the matrices. Fig.4(1) shows the micrograph of Pani-SO_4^{2-} and the distribution of size is not uniform and the particle size varies and the chain formation is clearly visible from the micrograph. The Pani-SO_4^{2-} also exhibits porous nature while the pores disappear in the composite structure. This illustrates that the nanocomposites are intercalated into the structure of polymer. It is shown in Fig.4(2) that the TiO_2 particles are well dispersed on the polymer matrix and coated the polymer uniformly with an average particle size. The distribution size is uniform but at some places it has formed agglomerates. Fig.4(3) shows that $CdTiO_3$ particles are also well dispersed on the polymer matrix. It is concluded that the homogenity of the composites is significantly improved by using the surface functionalized of TiO_2 and $CdTiO_3$ particles. This result is well supported by FTIR spectral data and XRD patterns.

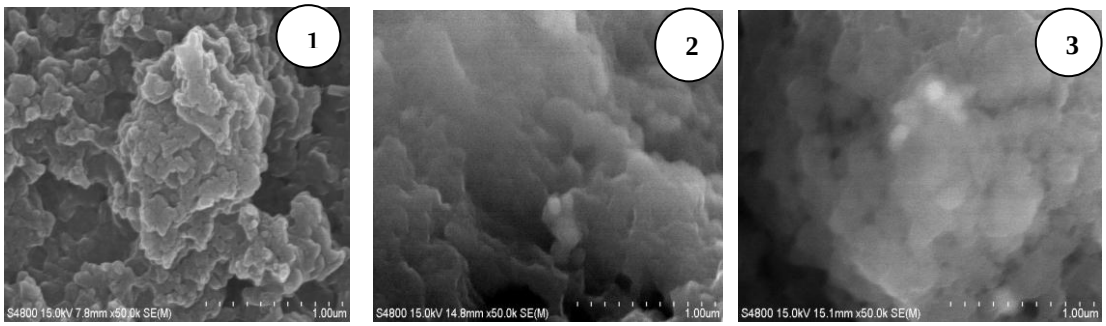

Fig.4 SEM Photographs for
(1) Pani-SO_4^{2-}; (2) Pani-SO_4^{2-}/TiO_2 and (3) Pani-SO_4^{2-}/$CdTiO_3$

Study of Antimicrobial Activity of Pani-SO_4^{2-}/$CdTiO_3$

The antimicrobial activities of the synthesized compounds were evaluated using the modified Kirby-Bauer disc diffusion method [36] against tested strains of Gram positive and Gram negative bacteria; then the activities of the most efficient compounds against the tested strains were further investigated. It is clear from the data that, the antibacterial activities of Pani-SO_4^{2-}/$CdTiO_3$ nanocomposite microspheres have good effects than Pani-TiO_2 and Pani- SO_4^{2-}. It can be used in antibacterial coating in water environment against bio-corrosion. Table 3 represents the antibacterial activity of PINC samples for various bacteria in a well diffusion assay. Results showed that Pani-SO_4^{2-}/$CdTiO_3$ demonstrated excellent antimicrobial activity against a range of bacteria. The diameter of inhibition zone reflects magnitude of susceptibility of microbes. The strains susceptible to Pani-SO_4^{2-}/$CdTiO_3$ exhibited larger zone of inhibition, whereas resistant strains exhibit smaller zone of inhibition for Pani-SO_4^{2-}/TiO_2 and Pani-SO_4^{2-}. According to zone inhibition *Enterobacter sps* has less inhibiton than other bacterial strains for Pani-SO_4^{2-}/$CdTiO_3$.

Table 3: Zone Inhibition data for polymer samples

Organisms	Zone of Inhibition (mm)-Media: Muller Hinton Agar				
	Chloramphenicol	Pani-SO_4^{2-}	Pani-SO_4^{2-}/TiO_2	Pani-SO_4^{2-}/$CdTiO_3$	NMP (NC)
E. coli	23.0	06.0	06.0	14.01	6.0
Pseudomonas aeroginosa	23.0	10.0	16.0	17.01	6.0
S. aureus	22.0	06.0	06.0	10.00	6.0
Proteus mirabilis	22.0	06.0	06.0	14.00	6.0
Klebsiella	24.0	18.0	18.0	17.00	6.0
Enterobacter sps	20.0	10.0	06.0	06.00	6.0
Chromobacter	30.0	16.0	19.0	18.00	6.0
Proteus vulgaris	21.0	06.0	06.0	15.00	6.0

CONCLUSION

The present study indicates the possibility of formation of an electronically conducting composite of environmentally stable conducting polymer like Pani and incorporated inorganic semiconductor TiO_2 and binary metal oxide of $CdTiO_3$. The polymerization yields are increased due to incorporation of nanoparticles. The growth of polymerization and conductivity are also enhanced. The incorporation of metal oxide is confirmed by EPR, UV-Visible, FTIR and XRD spectral studies. The FTIR studies also suggested the occurrence of chemical interaction between Pani and incorporated inorganic semiconductor of TiO_2 and bimetal oxide of $CdTiO_3$. The enhancement of conductivity has been attributed to the increase in the degree of crystallinity of Pani due to uncoiling/stretching of polymeric chain. The crystal structure and surface morphology of the polymer nanocomposites were revealed by XRD and SEM studies.

ACKNOWLEDGEMENT

The authors acknowledge the Institutes, CECRI, Karaikudi, STIC, Cochin, VHNSNC, Viruthunager and Vivek laboratories, Nagercoil for the characterizations and useful discussions.

CONFLICT OF INTEREST

The authors confirmed that there is no conflict of interest for this research paper.

REFERENCES

1. Ponzio EA, Benedetti TM, Torresi RM. Electrochemical and morphological stabilization of V_2O_5 nanofibers by the addition of polyaniline. Electrochim Acta 2007; 52(13): 4419-4427.
2. Malta M, Torresi RM. Electrochemical and kinetic studies of lithium intercalation in composite nanofibers of vanadium oxide/polyaniline. Electrochim Acta 2005; 50(25): 5009-5014.
3. Karim MR, Yeum JH, Lee MS, Lim KT. Preparation of conducting polyaniline/TiO_2 composite submicron-rods by the γ-radiolysis oxidative polymerization method. React Funct Polym 2008; 68(9): 1371-1376.
4. Karim MR, Lee CJ, Park YT, Lee MS. SWNTs Coated by Conducting Polyaniline: Synthesis and Modified Properties. Synth Met 2005; 151(2): 131-135.
5. Sudha JD, Sivakala S, Prasanth R, Reena VL, Nair PR. Development of electromagnetic shielding materials from the conductive blends of polyaniline and polyaniline-clay nanocomposite-EVA: Preparation and properties. Compos Sci Technol 2009; 69(3): 358-364.
6. Saxena V, Malhotra BD. Prospects of conducting polymers in molecular electronics. Curr Appl Phys 2003; 3(2-3): 293-305.
7. Li Q, Zhang C, Li J. Photocatalysis and wave-absorbing properties of polyaniline/TiO_2 microbelts composite by in situ polymerization method. Appl Surf Sci 2010; 257(3): 944-948.
8. Shang M, Wang W, Sun S, Ren J, Zhou L, Zhang L. Efficient Visible Light-Induced Photocatalytic Degradation of Contaminant by Spindle-like PANI/$BiVO_4$. J Phys Chem C 2009; 113 (47): 20228 -20233.
9. Liu XX, Zhang L, Li YB, Bian LJ, Huo YQ, Su Z. Electrosynthesis of Polyaniline SiO_2 Composite at high pH in the Absence of Extra Supporting Electrolyte. Polym Bull 2006; 57(6): 825-832.
10. Manjunath S, Koppalkar AK, Ambika Prasad MVN. Dielectric Spectroscopy of Polyaniline/Stanic Oxide (PANI/SnO_2) Composites. Ferroelect 2008; 366(1): 22-28.
11. Singh N, Kulkarni MV, Lonkar SP, Viswanath AK, Khanna PK. CdS/Polyaniline Nanocomposites: Synthesis and Characterization. Synth React Inorg Met Org Chem 2007; 37(3): 153-159.
12. Li G, Zhang C, Peng H, Chen K. One-Dimensional V_2O_5@Polyaniline Core/Shell Nanobelts Synthesized by an In situ Polymerization Method. Macromol Rapid Commun 2009; 30(21):1841-1845.
13. Huang X, Wang G, Yang M, Guo W, and Gao H. Synthesis of polyaniline-modified Fe_3O_4 /SiO_2 /TiO_2 composite microspheres and their photocatalytic application. Mater Lett 2011; 65(19-20): 2887-2890.
14. Song X, Yan C, Huang S, Zhang M. Synthesis of Mesoporous Polyaniline-TiO_2 Composite Microspheres for Gas Sensing Application. Adv Mater Res 2013; 750: 1098-1103.
15. Somani PR, Marimuthu R, Mulik UP, Sainkar SR, Amalnerkar DP. High Piezoresistivity and its Origin in Conducting polyaniline/TiO_2 composites. Synth Met 1999; 106(1): 45-52.
16. Parveen A, Roy AA. Effect of Morphology on Thermal Stability of Core-shell Polyaniline/TiO_2 Nanocomposites. Adv Mater Sci 2013; 4(9): 696-701.
17. Hu T, Shan S, Yang S, Jiang L. One-Step Synthesis and Antibacterial Properties of Polyaniline/TiO_2 Nanocomposites. Adv Mater Res 2012; 534: 78-81.
18. Jiang J. Facile Synthesis and Characterization of Polyaniline/$NiFe_2O_4$ Nanocomposite in w/o Microemulsion. J Macromol Sci Phys 2008; 47(2): 242-249.
19. Dexmer J, Leroy CM, Bockov R. Vanadium Oxide-PANI Nanocomposite-Based Macroscopic Fibers: 1D Alcohol Sensors Bearing Enhanced Toughness. Chem Mater 2008; 20(17): 5541-5549.

20. Kaushik A, Khan R, Gupta V, Malhotra BD, Ahmad S, Singh SP. Hybrid Cross-Linked Polyaniline-WO_3 Nanocomposite Thin Film for NOx Gas Sensing. J Nanosci Nanotechno 2009; 9(3): 1792-1796.
21. Gurunathan K, Amalnerkar DP, Trivedi DC. Synthesis and characterization of conducting polymer composite (PAn/TiO_2) for cathode material in rechargeable battery. Mater Lett 2003; 57: 1642-1648.
22. Safenaz M, Reda, Sheikha M, Ghannam Al. Synthesis and Electrical Properties of Polyaniline Composite with Silver Nanoparticles. Adv Mater Phy Chem 2012; 2(2): 75-81.
23. Pant HC, Patra MK, Nagi SC, Bhatia A, Vadera SR, Kumar N. Studies on Conductivity and Dielectric Properties of Polyaniline-Zinc Sulphide Composites. Bull Mater Sci 2006; 29(4): 379-384.
24. Pawar SG, Patil SL, Chougule MA, Raut BT, Jundale DM, Patil VB. Polyaniline: TiO_2 Nanocomposites: Synthesis and Characterization. Archiv Appl Sci Res 2010; 2(2): 194-201.
25. Chen SA, Lee HT. Polyaniline Plasticized with 1-methyl-2-pyrrolidone: Structure and Doping Behavior. Macromol 1993; 26(13): 3254-3261.
26. Cao Y, Smith P, Heeger AJ. Spectroscopic Studies of polyaniline in Solution and in Spin-cast Films. Synth Met 1989; 32(3): 263-281.
27. Laska J, Widlarz J. Spectroscopic and Structural Characterization of Low Molecular Weight Fractions of Polyaniline. J Polym 2005; 46(5): 1485-1495.
28. Zeng XR, Ko TM. Structure-conductivity relationships of iodine-doped polyaniline. J Polym Sci Part B: Polym Phys 1997; 35(13): 1993-2001.
29. Cheng DM, Ng SC, Chan HSO. Morphology of Polyaniline Nanoparticles Synthesized in Triblock Copolymers Micelles. Thin Solid Films 2005; 477(1-2): 19-23.
30. Alam M, Ansari AA, Shaik MR, Alandis NM. Optical and Electrical Conducting Properties of Polyaniline/Tin oxide Nanocomposite. Arab J Chem 2013; 6: 341-345.
31. Park NG, Ryu KS, Park YJ, Kang MG, Kim DK, Kang SG, Kim KM, Chang SH. Synthesis and electrochemical properties of V_2O_5 intercalated with binary polymers. J Power Sources 2002; 103(2): 273-279.
32. Dimitriew OP. Origin of the Exciton Transition Shift in Thin Films of Polyaniline. Synth Met 2001; 125(3): 359-363.
33. Boyer MI, Quillard S, Rebourt E, Louarn G, Bulsson JP, Monkman A, Lefrant S. Vibrational Analysis of Polyaniline: A Model Compound Approach. J Phys Chem B 1998; 102(38): 7382-7392.
34. Athawale AA, Deore BA, Kulkarni MV. Spectroscopic and Electrochemical Properties of Poly (2, 5 dimethyl aniline) Films. Mater Chem Phys 1999; 60(3): 262-267.
35. Pouget JP, Hsu CH, Mac Diarmid AG, Epstein AJ. Structural investigation of metallic PAN-CSA and some of its derivatives. Synth Met 1995; 69(1-3): 119-120.
36. Bauer AW, Kirby WM, Sherris C, Turck M. Antibiotic susceptibility testing by a standardized single disk method. Am J Clin Pathol 1996; 45(4): 493-496.

Cite this article as:
P. Suja Prema Rajini, V. S. John, R. Murugesan. Synthesis, Characterization and Anti-Microbial Activities on Polyaniline-$CdTiO_3$ Nanocomposite. J Pharm Chem Biol Sci 2017; 5(3):221-230